CORE MOVEMENT DURING PROCESSING OF SANDWICH PANELS

Duncan J. Pawson, Göran Fernlund

Composites Research Network
Department of Materials Engineering
The University of British Columbia
309-6350 Stores Road
Vancouver, BC, Canada V6T 1Z4

ABSTRACT

Core movement, also known as core crush, plagues sandwich panel fabrication as it renders the part unfit for service and must be scrapped. Much of the current research on this matter has focused on material factors, such as improving frictional resistance by tailoring fiber architecture and resin systems. However, a complete understanding of the problem from a processing perspective is still lacking. It is uncertain how processing conditions affect core movement. In particular, the manner in which core movement progresses is not well documented. As a result, methods for mitigating core movement are largely empirically based.

The focus of this paper is to better understand the factors influencing core movement during processing of sandwich panels. This paper evaluates the role parameters such as temperature and pressure play in dictating core movement. Moreover, specific ply movement is investigated, providing a better understanding of the mechanics of the problem. Experiments are conducted using a novel approach wherein core movement is measured and filmed in-situ within an autoclave using embedded sensors and an autoclavable camera.

1. INTRODUCTION

Sandwich panels are widely used in engineering applications, particularly in the aerospace industry. The benefit being that they allow for improved bending stiffness without compromising weight, similar to an I-beam. They have been incorporated in aircraft structures for nearly eighty years, with the first major use of sandwich panels introduced in the early 1940s during construction of the de Havilland Mosquito [1]. Composite sandwich panels are often manufactured using carbon or glass fiber reinforced polymers (CFRP and GFRP respectively) as the facesheets and Nomex honeycomb as the core.

As with many composite parts, sandwich panels are typically cured under external pressure in an autoclave. This presents a challenge, as the core often cannot withstand the high pressure and will collapse inward in its weak, lateral direction. This problem is often referred to as core crush or core movement. To prevent confusion with core crush in the through-thickness direction, the term core movement shall be used. Core movement is often extreme and visible by the naked eye. Deformed panels are irreparable and must be scrapped, making it one of the costliest

SAMPE Conference Proceedings. Charlotte, NC, May 20-23, 2019. Society for the Advancement of Material and Process Engineering – North America.

manufacturing problems in composites fabrication [2]. The problem is so pervasive that processing methods are often altered to prevent core movement [2], [3]. This may include processing the parts at lower pressures than a traditional laminate. Moreover, specific tools and layup methods are used to mitigate the risk. Tie downs are a common procedure wherein specific plies are restrained from moving, so to prevent deformation of the core itself. The idea being that if the friction between the core and immediate plies is relatively high, then by restraining ply movement, core movement is also prevented.

Much of the research on core movement has focused on the material aspect of the phenomena. For example, looking at the frictional resistance of various prepreg systems [2]–[4]. However, there is a lack of fundamental knowledge regarding the mechanisms involved in the core movement process. Moreover, the processing conditions under which the phenomenon occurs is not well defined. Therefore, methods to mitigate core movement are often based on empirical notions. There have been attempts to develop basic mechanical models for core movement [2], [4], however, these have yet to be validated. This calls for a science based approach to understanding the driving factors involved in core movement during the processing of sandwich panels. The work presented here is focused on the effect temperature plays in dictating core movement and the benefit of using in-situ data capture to study the phenomenon.

1.1 Honeycomb Mechanics

Nomex honeycomb is manufactured by expanding sheets of glued paper strips or ribbons. The structure itself is anisotropic as seen in Figure 1. The in-plane dimensions of a honeycomb structure refer to the X_1-X_2 plane. The out-of-plane or through-thickness dimension is the X_3 direction as shown in the figure [5], [6]. The X_2 direction is known as the ribbon (L) direction since it follows the direction of the glued ribbons. Correspondingly, the X_1 direction is known as the non-ribbon (W) direction. For the sake of consistency, the terms L and W will be used to refer to the X_2 and X_1 direction respectively.

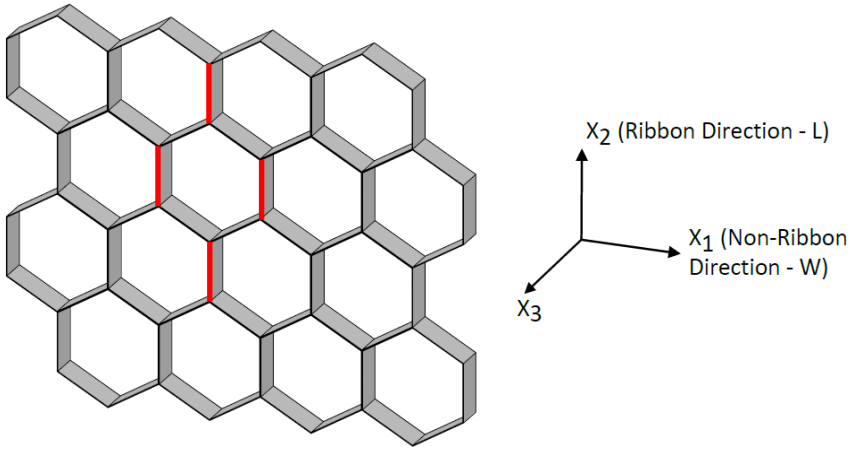

Figure 1: Hexagonal honeycomb structure. Glue lines are present in the ribbon direction as represented by the red lines.

While the functional loading direction of honeycomb is in the stiff, X_3 direction [6], it is in-plane, compressive loads that lead to core movement. In-plane compression of honeycomb

results in three distinct deformation phases. They are, in order of progression: I - bending, II - collapse, and III - densification [5], [7]–[10]. Bending constitutes a linear elastic regime wherein there is an initial constant rise in the stress strain curve. Cellular collapse may be the result of elastic buckling, formation of plastic hinges, or fracture of the cell walls. The manner in which collapse occurs is material dependent. It is characterized by a plateau region on the stress-strain curve, wherein deformation occurs under relatively constant stress due to failure of the cellular structure. Finally, densification occurs when opposing cell walls begin to touch. This is marked by an exponential rise in stress, as the cells close up and the structure increases in density. A typical stress-strain curve for an elastomeric honeycomb is shown in Figure 2 [5], [11].

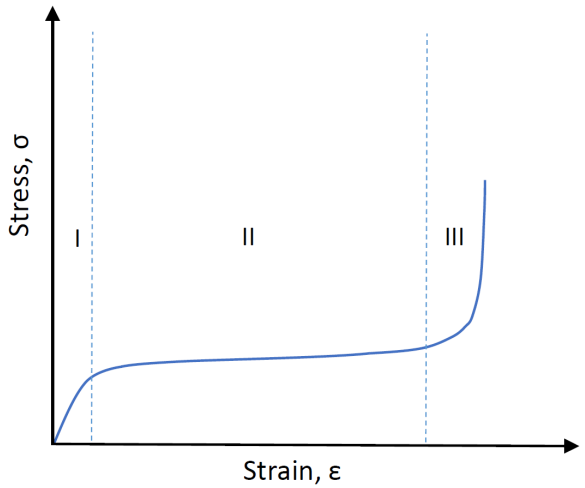

Figure 2: Typical stress-strain curve for an elastomeric honeycomb undergoing in-plane compression. I: Bending - linear elastic bending of cell walls, II: Collapse (plateau region) - constant stress as cells fail, III: Densification - cell walls touching. Figure adapted from [5]**.**

1.2 Inter-ply friction

When the inter-ply shear force exceeds the inter-ply friction, relative movement of plies occurs. That is, the plies yield or slip. This is an important concept, as ply slippage can dictate the extent of core movement [2], [4]. Throughout the processing cycle, a laminate may transition through different lubrication regimes, altering the dominant friction mechanism [12], [13]. For example, at low temperatures, the plies are separated by a resin film of considerable thickness wherein hydrodynamic lubrication dominates. Upon heating however, resin viscosity drops and fiber-fiber contact increases. This results in a boundary lubrication regime wherein coloumb friction dominates. Initially, this decreases the inter-ply friction due to a drop in viscosity. However, after reaching a minimum value, friction increases slightly due to fiber intermingling [4], [12]–[14].

Hydrodynamic and coloumb friction are represented by the following equations [12]:

$$Hydrodynamic\ Friction: \tau = \frac{\eta}{d} v \qquad [1.1]$$

Where, τ is resistive shear stress (friction), η is viscosity, d is film thickness, and v is relative speed between plies.

$$Coloumb\ Friction: F = \mu N \quad [1.2]$$

Where, F is the friction force, μ is the coefficient of friction, and N is the normal force.

1.3 Core Movement Process

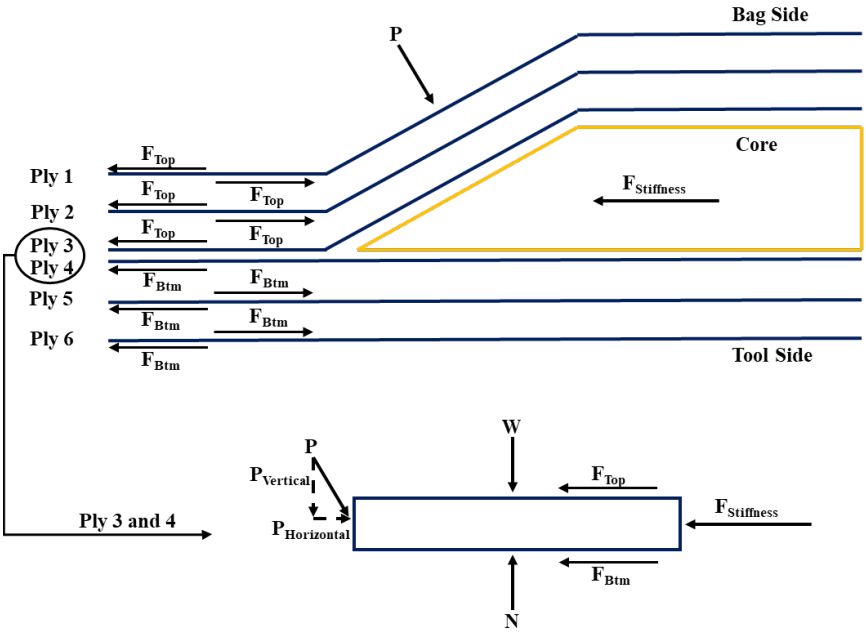

Figure 3: FBD of sandwich panel demonstrating forces involved in core movement. Figure adapted from [2]**.**

Core movement occurs when the lateral force acting on the panel exceeds the resistive forces of the panel. These resistive forces are a combination of the core stiffness and the inter-ply friction [2], [4]. Hsiao et al [2] summarizes the forces involved in core movement according to Figure 3. The applied force is transferred through the plies by a series of shear interactions, wherein the plies nearest the core experience the greatest shear force. Therefore, assuming the core and prepreg are well bonded, then in order for the core to deform, ply slippage must occur on the toolside and bagside surfaces. The manner in which ply slippage occurs is often assumed but not well understood, however. Hsiao et al postulate that slippage occurs across the interfaces of least friction, wherein the prepreg-bag interaction presents the highest friction. Therefore bagside slippage is assumed to occur across a prepreg-prepreg interface, whereas toolside slippage occurs across the prepreg-tool interface. This gives the condition for core movement as the following [2]:

$$F_{prepreg-prepreg} + F_{prepreg-Tool} + F_{stiffness} < P_{Horizontal} \cdot A \quad [1.3]$$

Where, A represents the cross-sectional area of the core.

2. EXPERIMENTATION

2.1 Materials

The prepreg used comprised of Cycom 970 epoxy resin with T300 3k fibers from Toray. The fibers were plain weave, standard twist, carbon fabric. The nominal resin content is 40 % by weight and contains added toughners. The material system is qualified to BMS8-256. It is a low flow, high temperature cure (177°C) material and is non self-adhesive, meaning a separate film adhesive must be placed between the prepreg and core. The film adhesive used was Metlbond 1515-4 which is co-cured with the prepreg. The core itself was HexWeb HRH-10-1/8-3.0 from Hexcel. It is a regular hexagonal Nomex honeycomb core with a cell size of 3.175 mm, density of 48.06 kg/m^3, and chamfer angle of 20°. Finally, Surface Master 905 from Solvay was used as the surfacing film on the tool, to provide a good surface and improve resin distribution on the base of the panel. It is also co-cured with the prepreg. A 12 mm, A36 steel tool was used for the experiments. The tool included stainless steel grit strips adhesively bonded and riveted on along its perimeter to allow for plies to be tied down.

2.2 Sensors

Two DS1000SUH linear variable displacement transducers (LVDTs) were used to track deformation of the panel in-situ. These were coupled with a 5M30 AC LVDT Conditioner to provide a calibrated analog output signal for displacement. The sensors were placed normal to the chamfer edge or radius in the L and W direction. In addition, one to two embedded pressure sensors were surgically placed in the core at the chamfer radius to track in-core pressure fluctuations during core movement. Both bagside and toolside locations were tested with no differences seen. Finally, an autoclavable camera was setup to allow for real-time visualization of the core movement process. Due to the size of the part and field of view of the camera, the recording was restricted to one corner of the panel. Both the pressure sensors and camera were developed by Convergent Manufacturing Technologies Inc. The sensor setup is shown in Figure 5.

2.3 Layup

Figure 4 provides an illustration of the layup used. Each panel consisted of a layer of surfacing film, twelve individual prepreg plies, one core, and two layers of film adhesive. The surfacing film was the first layer against the tool, followed by four prepreg plies. Film adhesive was then centered on the laminate and the core was centered on the film adhesive. Pressure sensors were inserted in the core and then another layer of film adhesive was draped over the core. A small cutout in the film adhesive was made around the pressure sensors to prevent intrusion into the sensors during cure. Four layers of filler plies were placed around the core in a pinwheel design, to allow for a smooth edgeband transition. The first two filler plies were butted against the core with the following two plies extending 6.35 mm and 12.7 mm up the core edge respectfully. Four, full length prepreg plies were draped over the whole structure. The film adhesive layers extended 12.7 mm past the core edge.

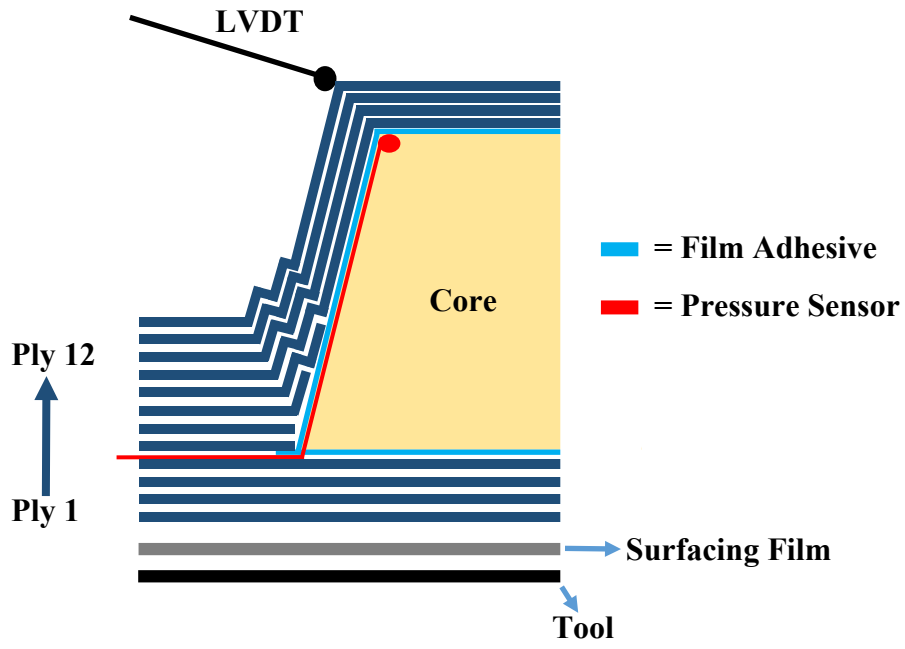

Figure 4: Sandwich panel layup

Once the layup was finished, PTFE release film was placed on the prepreg and breather cloth surrounded the entire panel. The part was then vacuumed bagged with pleats extending along the edgeband transitions to prevent bridging. Exact debulk time was not measured, but was limited to a few minutes.

2.4 Cure cycle

Three test panels were built according to the layup described. Each were processed at different temperatures, namely 95°C, 120°C, and 180°C. Heating was applied at a rate of 5°C/min, until the specified hold temperature, after which pressure application began. In each case, autoclave pressure was ramped up in steps of 103 kPa (~ 1 atm) up to 621 kPa gauge. Each pressure hold lasted for one minute until maximum pressure was achieved, which was held for three hours to allow the part to cure. In the case of the 95°C and 180°C samples, after one minute at maximum pressure, the hold temperature was changed to 120°C for final cure. At 103 kPa gauge, the vacuum bag was vented to atmospheric pressure. In addition to the three test panels, a fourth control panel was manufactured using single tie down plies. That is, the first plies above and below the core were restrained using the grit strips on the tool. This was done to prevent core movement. The control panel was processed at 120°C according to the same procedure as the test panels. RAVEN models [15] were used to calculate the resin viscosity of each sample throughout the cure cycle.

2.5 In-situ data

Data from the LVDT and pressure sensors were recorded real time using LabVIEW and later analyzed with MATLAB. A typical output is shown in Figure 6. Note that only one LVDT and pressure sensor is shown for clarity. The sudden early rise in vacuum pressure corresponds to venting of the vacuum bag. This is followed by a rise in in-core pressure. Considerable noise is

often seen in the pressure sensors once deformation is apparent. In-situ sensor data and video footage were synchronized to allow for an understanding of the exact processing conditions during each stage of core movement. Deformation seen in the control panel test was taken to represent deformation of the breather cloth, so to decouple core movement from breather displacement.

Core movement was broken into two stages, onset and collapse. These correspond to elastic bending and collapse of the honeycomb structure, respectively, as shown in Figure 2. Onset was defined as the first point of observable movement in both the video footage and LVDT data. This is represented in the LVDT data as the location where the displacement pattern of the panel deviates from that of the breather cloth, as observed during the control test. Collapse was defined as the point of obvious, continuous deformation. That is, the deformation proceeds rapidly at a relatively constant rate, independent of pressure holds.

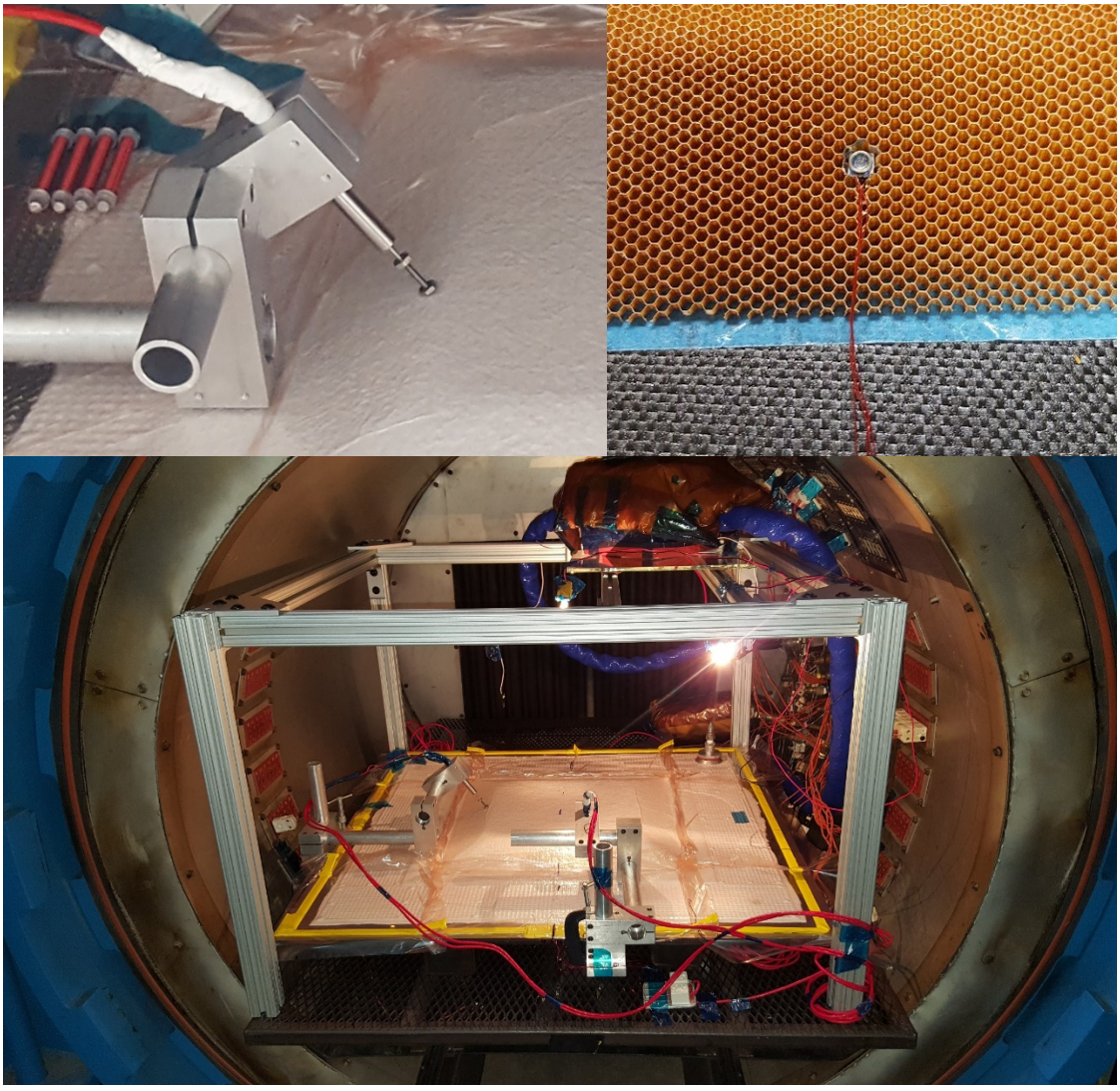

Figure 5: Test setup, showing in-situ sensors. Top left is an LVDT sensor, top right is an in-core pressure sensor, and the bottom is the full setup in the autoclave with the camera mounted above the panel.

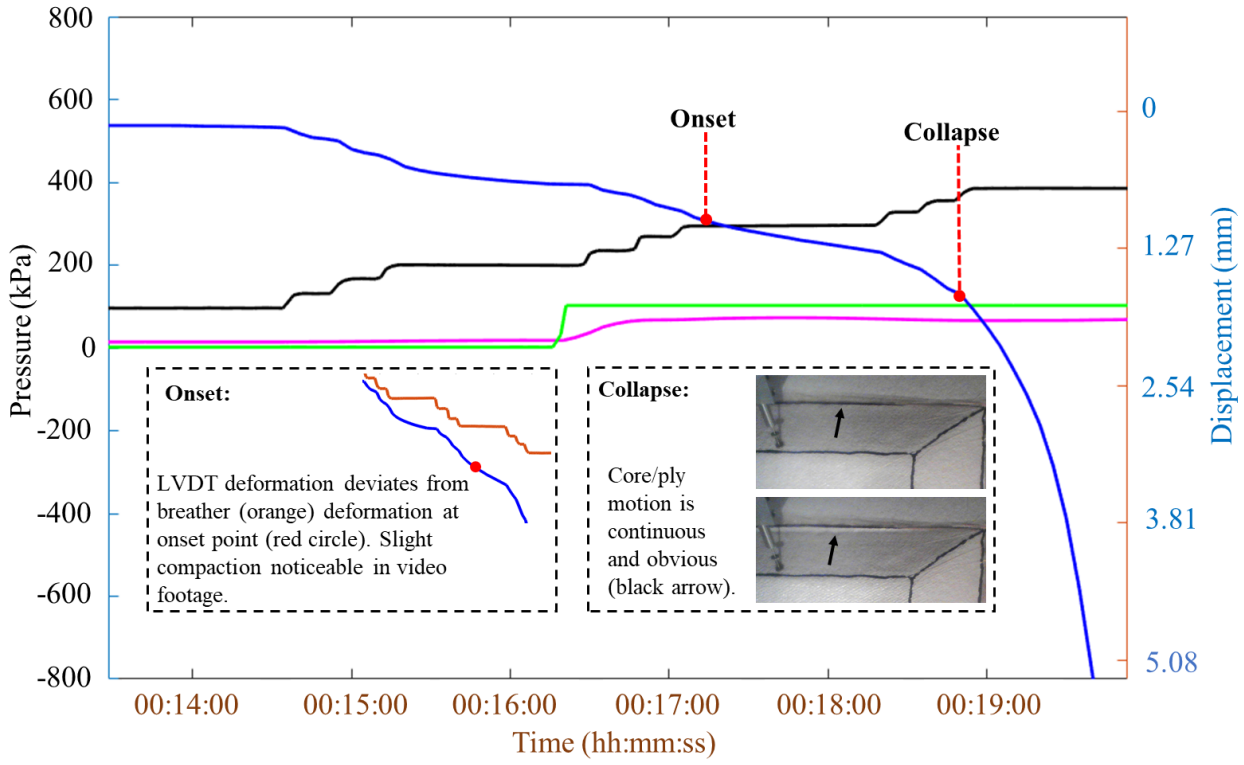

Figure 6: Data output from in-situ sensors. The colour scheme is as follows: black - autoclave pressure, blue – LVDT sensor, purple – in-core pressure sensor, green - vacuum pressure.

2.6 Post cure data

Following cure, panels were scanned using a coordinate measuring machine to obtain the surface topography. From this, thickness changes across the samples could be tracked to get an idea of ply movement. In addition to scanning, the panels were sectioned through-thickness along the L and W direction. The cut samples were polished allowing for individual plies to be observed via microscopy. A digital microscope was used to track the location each ply, so that individual ply movement could be determined.

3. RESULTS

3.1 Effect of temperature/viscosity on core movement

The net pressure at onset and collapse of the three tests are shown in Figure 7A. The net pressure is taken as the absolute external pressure acting on the part minus the pressure within the vacuum bag. The failure pressure at onset is relatively constant at 190 kPa between the 95°C and the 180°C samples. However, at 120°C the pressure to cause failure drops slightly to 170 kPa. This difference becomes more apparent at collapse, where the 95°C and 180°C samples fail around 267 kPa, yet the 120°C sample fails at 200 kPa. This drop in failure pressure is associated with a drop in viscosity below 10 Pa·s (Figure 7B). Interestingly, above 20 Pa·s, resistance to movement seems unaffected by changes in viscosity. This brings about the idea, that even for relatively low-viscosity material systems [12], the chance of panel deformation due to core movement remains the same for low versus high temperature processing. In other words, methods for mitigating such

defects do not need to be tailored to the specific cure cycle, so long as the viscosity remains above 20 Pa·s.

The range of pressure between onset and collapse can be thought of as the critical zone, where operating within this range may lead to core movement. Exceeding this range is likely to result in drastic core movement. The 120°C sample shows a smaller critical zone, wherein pressure fluctuations exceeding 30 kPa could push the operating pressure from below the onset point up to collapse.

It should be noted that from the time of pressure application until the onset of core movement, the viscosity does not change for the 95°C and 120°C samples. However, the viscosity changes rapidly for the 180°C sample. At the time of pressure application the 180°C sample had a viscosity of 12 Pa·s. A few minutes later, the viscosity rose to 68 Pa·s during the onset of core movement, and was around 368 Pa·s by the time collapse occurred. These values are based on numerical simulations from RAVEN [15].

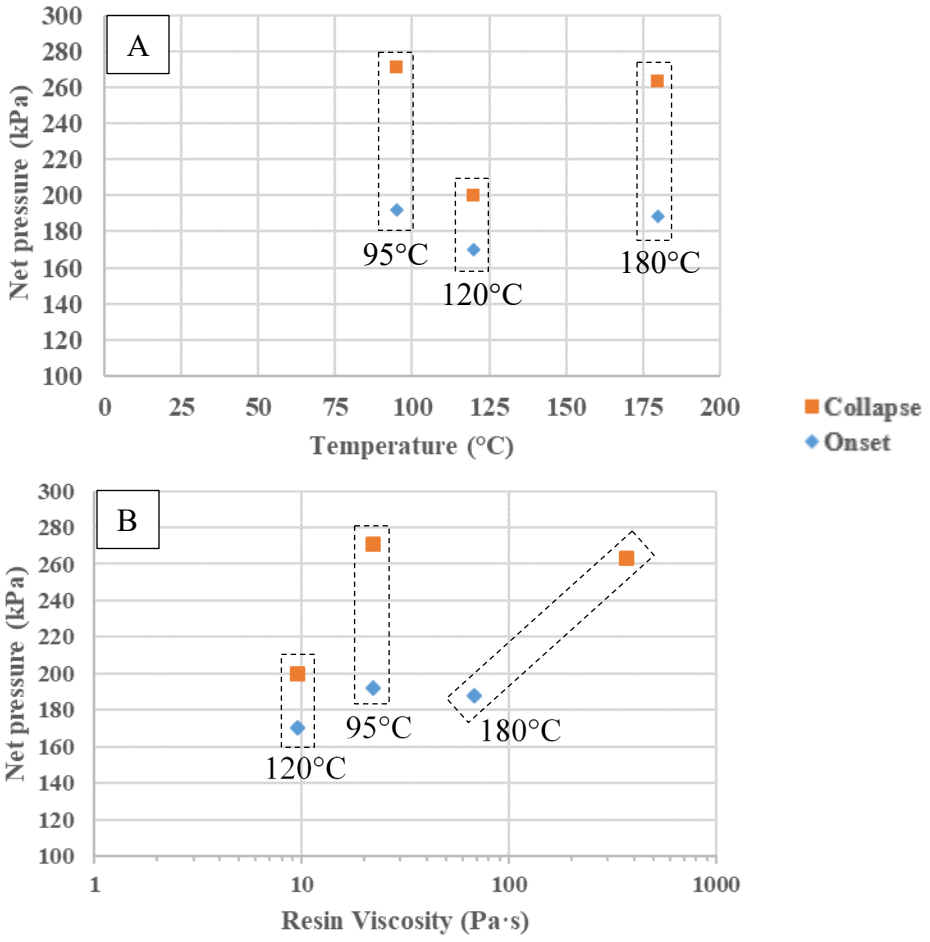

Figure 7: Net pressure to cause core movement with respect to (A) temperature and (B) resin viscosity. Note that the 180°C sample cures between onset and collapse, hence the increase in resin viscosity.

At first glance, Figure 7A seemingly implies that resistance to core movement follows a similar trend to inter-ply friction. Early on, during heating, friction is dictated by viscosity but eventually,

as viscosity is lowered, fiber-fiber contact dominates the response and friction stabilizes or increases slightly. This occurs before minimum viscosity [4]. However, as seen in Figure 7B, the lower failure pressure exhibited during the 120°C test corresponds to minimum viscosity, indicating hydrodynamic lubrication remains dominant throughout the cure cycle. It is possible, however, that depending on the temperature cycle, a viscosity lower than 10 Pa·s could be achieved wherein resistance to movement may in fact increase due to fiber intermingling.

It should be noted that the pressure to cause failure of the panels did not necessarily correspond to the extent of core movement. The 95°C and 120°C test panels showed similar levels of movement whereas the 180°C test panel showed less movement, albeit still drastic. Since temperature is increased to the hold temperature before pressure is applied, the part begins to cure somewhat before pressure application. In the case of the 95°C and 120°C test, the advancement of cure prior to pressure application is minimal. However, in the case of the 180°C test, crosslinking begins not long after pressure is applied. This effectively arrests the propagation of core movement not long after it begins. The onset of core movement and the collapse of the cellular structure is still apparent however.

3.2 Ply movement

While the pressure at the onset of core movement does not change drastically with temperature, there are noticeable patterns in the manner in which individual plies move. Gross movement patterns are highlighted by thickness changes in the panels as shown in Figure 8B. Lower processing temperatures result in more movement. However, as mentioned above, this is not indicative of the resistance to core movement, but rather demonstrates that viscosity remains low for a longer period of time at lower processing temperatures. In other words, core movement is allowed to continue rather that halting due to a relatively low degree of cure. This is heavily dependent on the nature of the cure cycle and is specific to the material system.

What is of particular interest is the shape of the thickness curves. Both the 120°C and 95°C samples display a gradual increase in thickness until the edgeband transition, whereas the 180°C case transitions immediately to the edgeband at some point. The 180°C panel shows less relative movement amongst plies, but rather a bulk movement of all plies. This is evident upon visual inspection of the cured panels, where the surfacing film is clearly seen up to the edgeband of the 180°C sample, indicating all plies have slid on this layer. This is however, not as clear in the other samples.

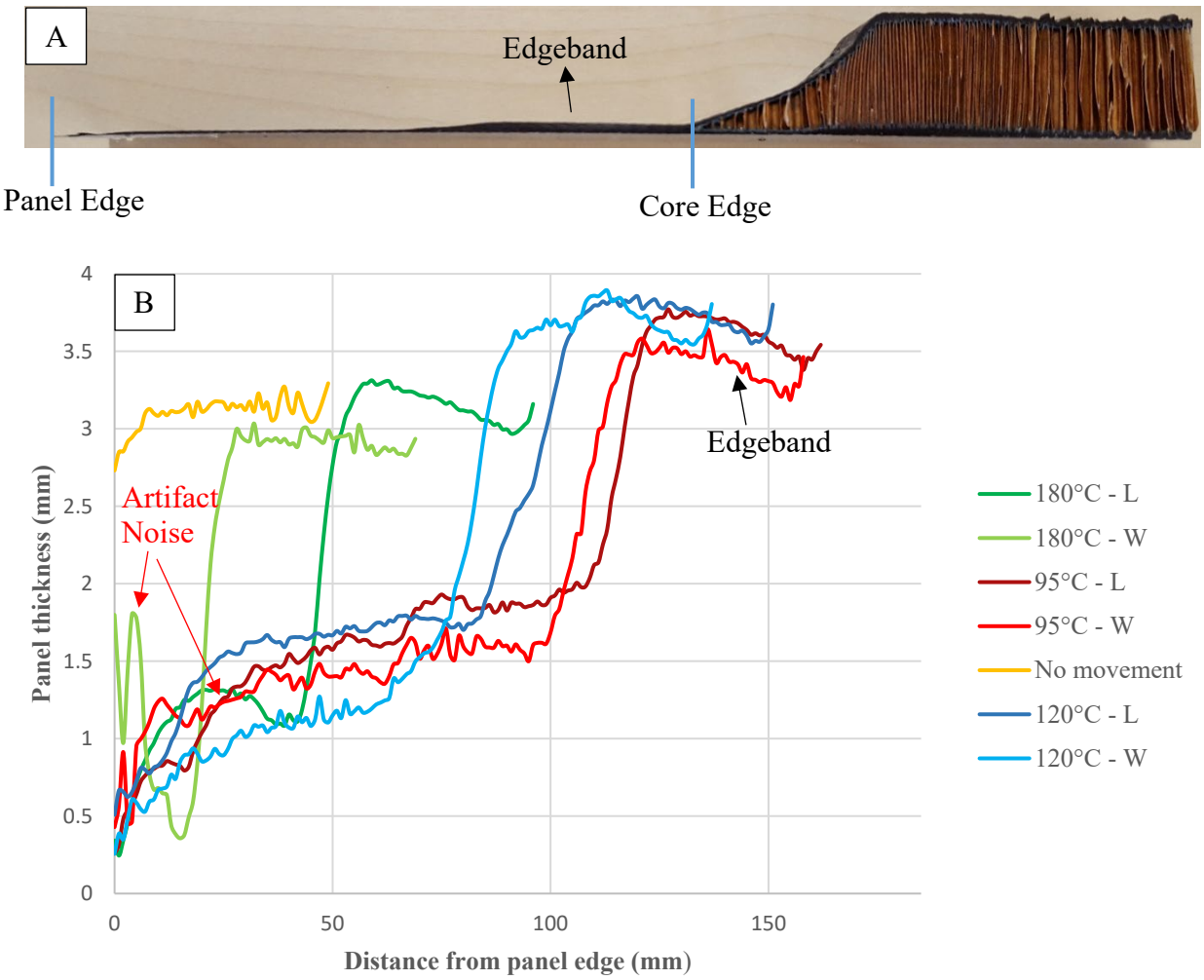

Figure 8: (A) Through-thickness section of 120°C sample in L direction. Panel thickness is measured between the blue lines and displayed in (B) for each sample. The control sample is represented by the "no movement" line.

The thickness variation across the panels gives an idea of the amount of plies located in a specific area. However, it is important to understand which specific plies are moving so to understand the core movement process from a mechanical perspective.

Figure 9 provides a detailed view into which plies pulled in with the core and the magnitude of this movement. Again, ply movement is displayed between the panel edge and core edge, as shown in Figure 8A. In each case the plies nearest the core (recall Figure 4) pull in the furthest, as would be expected. However, only in the 180°C case does the first ply (i.e. the ply directly against the surfacing film) pull in. It does so in both the ribbon and non-ribbon directions. Moreover, in the 180°C sample, in both the ribbon and non-ribbon directions, the magnitude of individual ply movement does not differ greatly amongst plies. This supports the notion that bulk motion of plies is favourable at higher temperatures. Similarly, as processing temperature is reduced, relative ply movement seems to increase between plies near the core edge and those further from the core edge.

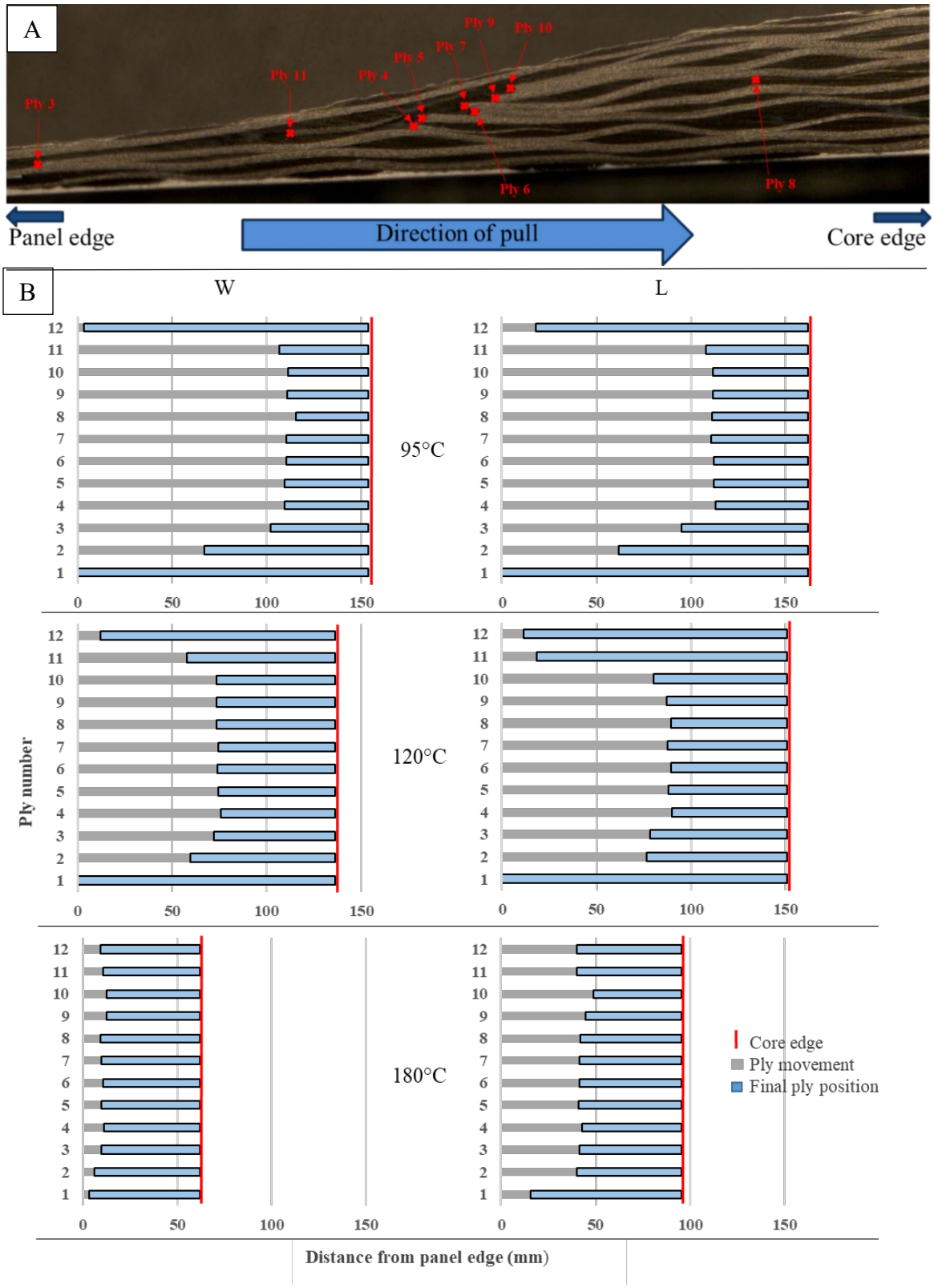

Figure 9: Specific ply movement profile. (A) Microscope image of 95°C - W showing individual plies. Plies drop off at different locations - marked by red 'X', indicating extent of movement. (B) Individual movement of plies and final position is plotted for each sample. Prior to movement, the core is 50.8 mm from panel edge.

In order for core movement to initiate, one bag-side and one-toolside ply must slip. This is dictated by the interfaces of least friction. It is impossible for plies further from the core to move without their counterparts nearer the core also moving, as inter-ply shear originates from the core. On the other hand, it is entirely possible that plies near the core could slip while those further away remain stationary. If the weakest interface were between the prepreg and peel ply (bagside), then slippage of this layer would result in all bagside plies moving equivalently. Similarly, if the surfacing film-prepreg interaction represented the weakest toolside interface, then all toolside plies would slip equivalently. On the other hand, if a prepreg-prepreg interface exhibited the lowest frictional resistance it would result in relative movement between the layers, with those nearest the core exhibiting the greatest movement. The problem can be thought of as deck of cards where the center of the deck is being pulled. If the top and bottom of the deck are not well supported (i.e. low friction), the whole deck may move. However, if the top and bottom are well supported (i.e. high friction), a cascading pattern will be observed with cards near the center pulling further than those towards the end. The results suggest that high temperature processing seems to shift towards the former scenario, whereas low temperature processing results in the latter case. One possible explanation is that the 180°C sample exhibited a higher degree of cure at the time of pressure application. This may have increased the inter-ply friction such that yielding of the prepreg-prepreg interface was no longer the root cause for slip. Rather, the peel ply and surfacing film now presented the weakest bagside and toolside interfaces, respectively, resulting in all plies sliding relative to these layers. It should also be noted that relative motion of plies increases hydrodynamic shear according to equation ([1.1). Therefore, it is possible that slippage occurred across a single ply interface, after which shear between the two layers increased, resulting in slippage of the other layer. This too, would result in a cascading pattern of ply movement, and is therefore a less likely scenario for the 180°C case.

Surprisingly, in all three samples the ribbon direction exhibits more deformation than the non-ribbon direction. This is more apparent the higher the processing temperature, with the 95°C sample displaying only minor differences in deformation. Interestingly, in-situ data indicates onset of failure occurs in both directions simultaneously. Although, at higher processing temperatures, collapse in the ribbon direction occurs at a notably faster rate. This may be attributed to the manner in which cell collapse occurs in the two directions. Under uniaxial loading in the L direction, Nomex honeycomb has been shown [11] to display a homogenous collapse of the cellular structure by buckling of members along the load path. Conversely, loading in the W direction results in a row-by-row collapse pattern by forcing together of members perpendicular to the load direction. Although under biaxial loading the pattern of deformation appears to be a combination of those seen in the uniaxial case [5], the homogenous buckling of cells in the L direction may present itself as a quicker or preferential mode of deformation once collapse begins. Alternatively, a buckling collapse pattern may allow for greater densification of the cellular structure.

4. CONCLUSIONS

The pressure to initiate core movement was similar amongst samples cured at 95°C and 180°C, corresponding to low and high temperature processing. The sample cured at 120°C showed a 10 % reduction in failure pressure at the onset of core movement. This difference was greater at collapse of the structure, with the 120°C sample collapsing at a pressure 25 % lower than the other

two samples. This correlates with a drop in viscosity below a threshold value; as viscosities above 20 Pa·s seem to play no role in altering the force required for core movement initiation. The concept of a critical zone to visualize failure pressure is a useful way to approach the problem, wherein the lower bound of failure pressure represents the onset of core movement and the upper bound represents collapse. Manufacturers should be weary to operate within or above the critical zone, unless proper core movement mitigation methods are taken. As shown, the critical zone varies in size depending on the processing conditions. Therefore, even small pressure fluctuations may have severe consequences.

The mechanical nature of inter-ply slip during core movement is affected by processing temperature. Panels cured at high temperature show a tendency for bulk ply motion during core movement, whereas panels processed at low temperature display more relative ply movement. The difference being slippage across the bagside/toolside interfaces versus slippage across a prepreg-prepreg interface. The interface of least friction is, therefore, dependent on processing temperature. This calls for an updated mechanical model which takes this into account. It should also be noted that panels processed without peel ply or surfacing film may exhibit different results.

In all three samples, the ribbon direction deformed more than the non-ribbon direction, despite that failure occurred in both directions simultaneously. This dissimilarity was more pronounced at higher processing temperatures.

In-situ data collection sheds light on a stage of the composite manufacturing process that is typically treated as a black box – the autoclave. The methodology presented here is not limited to core movement, but can be implemented in a wide array of processing scenarios. Techniques such as these can be used to investigate previously unanswered questions or simply act as a means of monitoring a part during processing. Novel, in-situ measurement techniques are therefore useful both from an academic and industrial perspective. Future work by the authors focusses on understanding the effect different layups have on core movement, through applying similar techniques as presented here.

5. REFERENCES

[1] Aktay, L., Johnson, A. F., and Kröplin, B. H., "Numerical modelling of honeycomb core crush behaviour," *Eng. Fract. Mech.*, vol. 75, no. 9, (2008): pp. 2616–2630. http://10.1016/j.engfracmech.2007.03.008

[2] Hsiao, H.M., Lee, S., and Buyny, R., "Core Crush Problem in the Manufacturing of Composite Sandwich Structures: Mechanisms and Solutions," *AIAA J.*, vol. 44, no. 4, (2006): pp. 901–907. http://10.2514/1.18067

[3] Pelton, T. L., Schneider, T. L., and Martin, R., "Material factors influencing composite part producibility in relation to prepreg frictional measurement," *Proceedings of Int. SAMPE Tech. Conf.* Long Beach, California, May 23-27, 1999. Society for the Advancement of Material and Process Engineering. Vol. 31: pp. 463–477.

[4] Martin, C. J., Seferis, J. C., and Wilhelm, M. A., "Frictional resistance of thermoset prepregs and its influence on honeycomb composite processing," *Compos. Part A: Appl.*

Sci. Manuf., vol. 27, no. 10, (1996): pp. 943–951. http://10.1016/1359-835X(96)00037-1

[5] Gibson, L. J. and Ashby, M. F., *Cellular solids: structure and properties*. Pergamon Press, 1988.

[6] Zhang, J. and Ashby, M. F., "The out-of-plane properties of honeycombs," *Int. J. Mech. Sci.*, vol. 34, no. 6, (1992): pp. 475–489. http://10.1016/0020-7403(92)90013-7

[7] Ashby, M. F., and Mehl Medalist, R. F., "The mechanical properties of cellular solids." *Metall. Trans. A*, vol. 14, no. 9, (1983): pp. 1755-1769. http://10.1007/BF02645546

[8] Chen, Q. and Pugno, N. M., "In-plane elastic buckling of hierarchical honeycomb materials," *Eur. J. Mech. A/Solids*, vol. 34, (2012): pp. 120–129. http://10.1016/j.euromechsol.2011.12.003

[9] Papka, S. D. and Kyriakides, S., "In-plane compressive response and crushing of honeycomb," *J. Mech. Phys. Solids*, vol. 42, no. 10, (1994): pp. 1499–1532. http://10.1016/0022-5096(94)90085-X

[10] Papka, S. D. and Kyriakides, S., "Experiments and full-scale numerical simulations of in-plane crushing of a honeycomb," *Acta Mater.*, vol. 46, no. 8, (1998): pp. 2765–2776. http://10.1016/S1359-6454(97)00453-9

[11] Heimbs, S., Schmeer, S., Middendorf, P., and Maier, M., "Strain rate effects in phenolic composites and phenolic-impregnated honeycomb structures," *Compos. Sci. Technol.* vol. 67, no. 13, (2007): pp. 2827–2837. http://10.1016/j.compscitech.2007.01.027

[12] Larberg, Y. R. and Åkermo, M., "On the interply friction of different generations of carbon/epoxy prepreg systems," *Compos. Part A: Appl. Sci. Manuf.*, vol. 42, no. 9, (2011): pp. 1067–1074. http://10.1016/j.compositesa.2011.04.010

[13] Erland, S., Dodwell, T. J., and Butler, R., "Characterisation of inter-ply shear in uncured carbon fibre prepreg," *Compos. Part A: Appl. Sci. Manuf.,* vol. 77, (2015): pp. 210–218. http://10.1016/j.compositesa.2015.07.008

[14] Ersoy, N., Potter, K., Wisnom, M. R., and Clegg, M. J., "An experimental method to study the frictional processes during composites manufacturing," *Compos. Part A: Appl. Sci. Manuf.*, vol. 36, no. 11, (2005): pp. 1536–1544. http://10.1016/j.compositesa.2005.02.010

[15] Convergent Manufacturing Technologies, 2019. <https://www.convergent.ca/>.